

# Formulation and Characterization of Alginate Beads with HPMC Containing Eugenol for pH Sensitive Release

Yasser Kessira, Souheila Touati, Djallel Bouzid\*

Laboratoire de Génie des Procédés pour le Développement Durable et les Produits de Santé  
 Ecole Nationale Polytechnique de Constantine, BP 75, A, Nouvelle Ville RP, Constantine, Algeria  
 djallel.bouzid@enp-constantine.dz

Eugenol is a natural phenolic compound with strong antimicrobial and antioxidant activity. Despite its benefits, its volatility and low stability limit its practical applications. To overcome this issue, it has been encapsulated in alginate beads via ionic gelation with  $\text{CaCl}_2$  as crosslinker. To enhance the sustained release and the swelling properties, a fixed amount of hydroxypropyl methylcellulose (HPMC) was incorporated into the formulation. Fresh beads with white colour exhibited two distinct shapes, spherical and teardrop, with sizes ranging between 2.53 and 3.30 mm. The effect of alginate and  $\text{CaCl}_2$  concentrations on the encapsulation efficiency (EE) was investigated, and it was found that the highest EE of 78.8 % was achieved with 2 % w/v alginate and 5 % w/v  $\text{CaCl}_2$ . Beads formulated with 4 % alginate and 7 % w/v  $\text{CaCl}_2$  showed an EE of 73 % while an increase in the EE from 55.6 % to 72.2 % was observed when the alginate concentration increased to 6 % w/v. Furthermore, the beads demonstrated selective swelling in buffer medium (pH 6.8) and maintained their structure in acidic medium (pH 1.2). Scanning Electron Microscopy (SEM) revealed the presence of nano/microscopic pores on the rippled surface of the beads, which may explain the swelling effect. These findings convey that eugenol encapsulation in alginate beads potentially provides a feasible approach for achieving sustained and targeted release in biotechnical and nutritional products while protecting it from degradation and other factors that could alter its effectiveness.

## 1. Introduction

Clove essential oil (CEO), obtained from *Eugenia caryophyllata*, is dominated by eugenol, which is responsible for its potent antimicrobial and antioxidant properties (Chaieb et al. 2007). Eugenol is used in foods and cosmetics and dental care for its antiseptic and pain-relieving properties (Pinto et al. 2009). Given its functional profile and a reported acceptable daily intake ( $\approx 2.5$  mg/kg body weight), eugenol remains a practical and promising prospect for further scientific exploitation (Gülçin 2011). Eugenol shares the usual drawbacks associated with essential oils, it is poorly soluble in water, and easily degradable by oxygen, light and heat (Sherry et al. 2013). Those limits reduce bioavailability and shorten functional lifetime, and the strong aroma or taste can be unwanted in some products (Jobdeedamrong et al. 2018). Encapsulation has been used to address these problems, systems such as emulsions, beads, films, liposomes, and inclusion complexes help stabilize volatile compounds, reduce evaporation, mask unpleasant sensory notes and enable controlled release (Kfoury et al. 2019).

A polysaccharide extracted from brown algae, alginate is a biocompatible and biodegradable polyelectrolyte that is composed of randomly linked  $\beta$ -D-mannuronic acid and  $\alpha$ -L-guluronic acid forming M blocks and G blocks, respectively (Ramos et al. 2018). Due to its high biocompatibility and biodegradability, it is one of the most widely used polyelectrolytes in beads formulation (Ward et al. 2005). Its ability to form gels in the presence of divalent cations, particularly  $\text{Ca}^{2+}$ , has been extensively exploited in the development of matrices for the controlled release of bioactive agents (Chen et al. 2012). Ionic gelation is a widely employed technique for alginate-based encapsulation. This technique involves the replacement of  $\text{Na}^+$  cations in a sodium alginate solution/emulsion with  $\text{Ca}^{2+}$  cations when it encounters a gelling bath of dissolved calcium chloride. The

crosslinked structure of the resulting matrix resembles an egg-box shape where the polymer chains form the box walls, and the ions linking them together are analogous to the eggs (Uyen *et al.* 2020).

The use of ionic gelation for the encapsulation of active substances including solids, essential oils, and cells has been extensively explored in various studies (Ahmed *et al.* 2013, Bowey *et al.* 2013, Bagheri *et al.* 2014, Hu *et al.* 2017). However, limited attention has been given to eugenol or CEO encapsulation using this method in the presence of HPMC. This latter could as a matter of fact improve the swelling properties, and yet only a scarce number of studies have been published on this topic (Soliman *et al.* 2013, Faidi *et al.* 2019, Radünz *et al.* 2019). The present study aims at evaluating the impact of several critical formulation parameters, such as needle size and position, alginate and CaCl<sub>2</sub> concentrations, on eugenol-loaded beads physical and chemical characteristics. This work does not aim to compare alginate-only and alginate-HPMC beads, but to investigate how formulation and process parameters influence the properties of eugenol-loaded beads within this hybrid matrix. This investigation serves as a pivotal foundation for the development of stable oil-loaded pH-sensitive beads with controlled and prolonged release properties that could be useful in food and biotechnical products.

## 2. Materials and methods

### 2.1 Beads preparation

Sodium alginate (Sigma-Aldrich) was dissolved in distilled water under magnetic stirring at room temperature to give the chosen concentrations. A fixed amount of HPMC (viscosity 40–60 cP, 2 % H<sub>2</sub>O; Alfa Aesar) was added to the alginate solution (1 % w/v HPMC) and stirred until fully dissolved. The alginate/HPMC mixture was sonicated for 30 min at ambient temperature to remove trapped air. For loaded beads, eugenol (pure; AIREL PHARMA) was added to the alginate/HPMC at 10 mg/mL. The blend was homogenized with a POLYTRON PT 2500 E at 8000 rpm for 5 min to form a fine emulsion. The emulsion was degassed in an ultrasonic bath for 30 min. Gelling baths were prepared by dissolving CaCl<sub>2</sub> dehydrate (VWR Chemicals) at the required amounts in deionized water. Alginate/HPMC solution or the eugenol emulsion (10 mL loaded into the syringe) were delivered dropwise into the CaCl<sub>2</sub> bath using an injection pump (Kelly Med KL-602). Needle height above the bath (6, 9, and 12 cm) and needle size (25 and 20-gauge needles) were screened to select the conditions that gave the desired bead size and shape. Upon contact with Ca<sup>2+</sup> the droplet surface gelled to form alginate beads, which were allowed to crosslink in the bath for 30 min, then collected by sieving and rinsed with distilled water to remove residues, then placed on Petri dishes and dried at room temperature for 48 h. All other reagents were analytical grade and purchased from Sigma-Aldrich.

### 2.2 Size, shape and surface morphology

Wet unloaded beads and both wet and dry eugenol-loaded beads were photographed using a digital camera. ImageJ software was used to determine diameters after calibration with a scale marker. The resulting data were processed with Origin for statistical fitting. In addition, bead morphology was investigated using optical microscopy (ZEISS AXIOIMAGER Z2m) and scanning electron microscopy (Philips XL-30 FEG). While optical microscopy gave an overview of beads topological features, SEM provided detailed images of the surface.

### 2.3 Encapsulation efficiency, loading capacity and storage stability

Encapsulation efficiency (EE) and loading capacity (LC) were determined by dispersing a known amount of dry beads in phosphate buffer (pH 6.8) for 3 min, followed by crushing in an agate mortar with ethanol (10 mL) to ensure complete extraction of eugenol. After centrifugation at 4000 rpm for 30 min (KL02A centrifuge), the supernatant was analysed by UV-visible spectrophotometry (UV-1800 Shimadzu) at 282 nm. Eugenol concentration was quantified using a calibration curve, which showed good linearity over the studied concentration range ( $y = 0.0188x + 0.0024$  with  $R^2 = 0.98$ ). Preliminary tests confirmed the absence of interference from alginate or HPMC at the selected wavelength. EE (%) was calculated as the ratio of encapsulated to initial eugenol, while LC (%) was calculated as the ratio of eugenol mass to bead mass. To assess stability, selected dry bead samples (F02, F07, F12) were stored in sealed containers at room temperature for 150 days, after which EE was re-measured. Retained eugenol (%) was calculated by comparing the EE of stored samples with that of freshly prepared beads. All experiments were performed in triplicate ( $n = 3$ ), and results are expressed as mean  $\pm$  standard deviation.

### 2.4 In vitro swelling and release study

Swelling and release were tested to simulate gastrointestinal pH conditions. Dry beads with the highest EE for each alginate concentration were placed in buffer solutions at pH 1.2, 6.8, and 7.4 at laboratory temperature ( $\approx 25$  °C). Swelling was monitored by photographing the beads in multi-compartment plates with scale indicators. Swelling was quantified as the percentage change in bead diameter relative to the initial dry state, with mean

values and standard deviations obtained from five independent measurements. For release studies, weighed samples of dry eugenol-loaded beads (F02, F07, F12) were immersed in pH 6.8 buffer under sink conditions. At set time intervals, 5 mL aliquots were withdrawn and replaced with fresh buffer to maintain constant volume. After liquid–liquid extraction with methylene chloride, eugenol concentration was quantified by UV-Vis spectroscopy against calibration standards. Cumulative release data are plotted as a function of time. Release kinetics were analyzed by fitting experimental data to first-order, Higuchi and Korsmeyer–Peppas models.

### 3. Results and discussion

#### 3.1 Blank, wet, and dry beads size analysis

Needle diameter and drop height were the main factors controlling bead size. Using the 20-gauge needle produced noticeably bigger beads (mean  $\approx$ 3.9–4.7 mm) (Figure 1a), while the finer needle yielded smaller beads ( $\approx$ 3.3–3.9 mm) (Figure 1b), which agrees with earlier work showing tip diameter sets the detached droplet volume and thus final particle size (Partovinia and Vatankhah 2019). Increasing the drop height tended to increase average diameter and broaden the size distribution, likely, because faster impacts deform droplets before gelation. Other studies have reported similar trends and argued that lowering dripping height is a simple way to reduce size and size variability (Abang *et al.* 2012). The finer (25-gauge) needle at the shortest tested distance (6 cm) where used for all subsequent formulations.

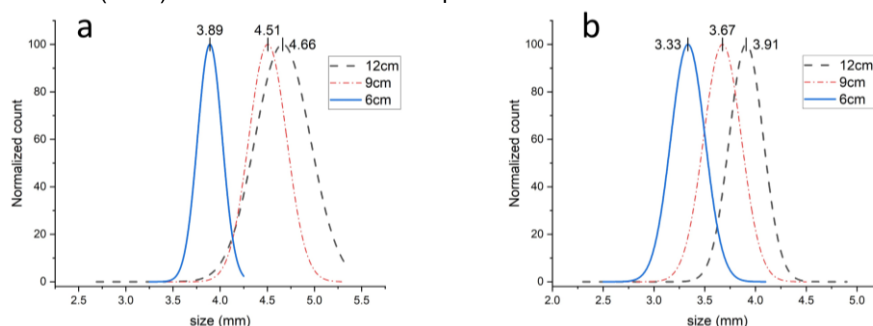


Figure 1: Size distribution of blank beads formulated by 20-gauge needle (a) and 25-gauge needle (b) at 3 distances: 6, 9, and 12 cm.

Table 1: Formulation conditions and measured properties of eugenol-loaded beads. n.d.: not determined; storage stability measurements were performed only for selected formulations (F02, F07, F12).

Sample	Alginate concentration (% w/v)	CaCl <sub>2</sub> concentration (% w/v)	Wet beads size (mm)	Dry beads size (mm)	Shrinking factor	EE (%)	LC (%)	EE (%) after storage
F01	2	3	2.81 ± 0.12	1.36 ± 0.04	2.06	66.2 ± 3.17	11.4 ± 1.17	n.d.
F02	2	5	2.53 ± 0.08	1.45 ± 0.09	1.74	78.8 ± 1.13	10.5 ± 0.55	74.3
F03	2	7	3.02 ± 0.14	1.44 ± 0.07	2.10	65.9 ± 1.53	9.4 ± 0.18	n.d.
F04	2	9	2.87 ± 0.11	1.55 ± 0.12	1.85	69.4 ± 4.34	9.3 ± 0.62	n.d.
F05	4	3	2.93 ± 0.07	1.29 ± 0.06	2.27	56.8 ± 2.15	7.3 ± 0.32	n.d.
F06	4	5	3.3 ± 0.16	1.27 ± 0.08	2.60	62.8 ± 2.06	7.2 ± 0.24	n.d.
F07	4	7	3.0 ± 0.09	1.41 ± 0.05	2.13	73.0 ± 1.5	6.6 ± 0.13	72.4
F08	4	9	3.15 ± 0.13	1.44 ± 0.06	2.19	62.6 ± 1.2	6 ± 0.11	n.d.
F09	6	3	3.1 ± 0.12	1.46 ± 0.16	2.12	55.6 ± 0.33	5.1 ± 0.03	n.d.
F10	6	5	3.13 ± 0.1	1.45 ± 0.09	2.16	58.6 ± 0.8	4.8 ± 0.07	n.d.
F11	6	7	3.03 ± 0.06	1.50 ± 0.07	2.02	67.9 ± 2.57	4.7 ± 0.19	n.d.
F12	6	9	3.0 ± 0.07	1.60 ± 0.13	1.88	72.2 ± 1.12	4.6 ± 0.07	70.9

Wet bead diameters fell between 2.5 and 3.3 mm, and two clear patterns stood out (Table 1). First, alginate and CaCl<sub>2</sub> concentrations influenced the mean bead size. At low CaCl<sub>2</sub> concentration (3 % w/v), increasing alginate content resulted in a slight increase in bead diameter. In contrast, at moderate-to-high CaCl<sub>2</sub> concentrations, the largest beads were obtained at 4 % w/v alginate. This indicates that solution rheology and crosslinking kinetics affect bead formation, although the initial droplet volume imposed by the nozzle remains the primary determinant of bead size (Lee and Mooney 2012). Second, low-polymer/low-crosslink runs tended to form aggregates, likely because slow shelling lets partially set droplets collide and fuse; by contrast, higher-viscosity and rapid surface gelation locked in non-spherical, often teardrop shapes (Davarcı *et al.* 2017). Dry beads

diameters ranged from 1.27 to 1.60 mm. For reproducible eugenol release, the best compromise is a window of moderate alginate with sufficient  $\text{CaCl}_2$  to avoid clustering but not so much that shapes become irregular.

### 3.2 Encapsulation efficiency, loading capacity and storage stability

EE across samples was reasonably high, ranging from 55.6 % to 78.8 % (Table 1), with formulation F02 (2 % w/v alginate, 5 % w/v  $\text{CaCl}_2$ ) having the highest EE of 78.8 %. LC varied roughly between 4.6 % and 11.4 %. EE reflected the balance between polymer concentration and crosslinking strength, moderate  $\text{Ca}^{2+}$  levels improved oil retention, while excessively strong gelling conditions reduced EE at low alginate content (Maes *et al.* 2019). Increasing alginate concentration reduced LC because the same oil amount represented a smaller fraction of the total bead mass (Benavides *et al.* 2016). The presence of HPMC likely contributed to retention by increasing pre-gel viscosity and forming a secondary polymer network within alginate, which limits oil diffusion during gelation. During processing, eugenol losses occurred mainly by diffusion into the gelling bath, visible as clouding, and by volatilization during air-drying explaining why experimental EE and LC were lower than theoretical values. Storage tests on three high-EE formulations (F02, F07, F12) stored at room temperature for 150 days showed good retention. Losses were small (less than 6 %), with F02 retaining 94.3 % and F07 99.2 % of initial EE (Table 1). This level of stability supports applications where multi-month shelf life is acceptable.

### 3.3 Loaded beads surface topology

Optical microscopy (Figure 2a) and SEM revealed that bead surface features were highly sensitive to alginate content and drying conditions. At low alginate levels (2 % w/v), dried beads showed ripples and flattened contact areas where they had touched during drying (Figure 2b). These patterns were not present immediately after gelation but developed as water loss and capillary stresses caused surface contraction and local collapse. Similar drying-induced corrugations have been reported in alginate gels, where the method of drying and bead packing strongly shape the final texture (Santagapita *et al.* 2011). SEM images (Figure 2c) confirmed that low-polymer beads had a porous outer layer with (pores size of  $\approx 1.61 \mu\text{m}$ ) and a relatively open internal structure, consistent with reduced crosslink density and greater susceptibility to collapse (Lee and Mooney 2012).

At higher alginate concentrations, beads dried with smoother surfaces or showed discrete bumps rather than fine rippling. The increased viscosity of the starting solution produced larger droplets that resisted rapid shape relaxation, while faster surface gelation “locked in” more stable geometries. These factors combined to reduce shrinkage and give a more uniform external appearance. These morphological differences are consistent with the observed swelling and release behavior; beads with more open and porous surfaces exhibited greater swelling and faster initial eugenol release, whereas smoother, denser surfaces promoted structural stability and slower release profiles. Overall, formulation and drying route jointly determine surface topology, which is a key parameter for both handling properties and functional performance of loaded beads.

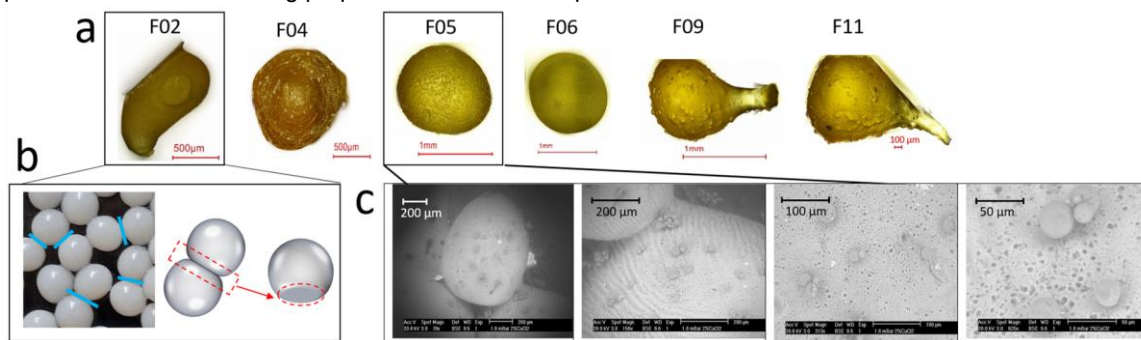


Figure 2: Optical microscopy photos of selected runs (a), Depiction of wet beads arrangement effect on deformation after drying (b), SEM photos of the microscopic topology (c).

### 3.4 Swelling behavior and in vitro release

The swelling behaviour of F02, F07, and F12 beads in buffer media of pH 1.2, 6.8 and 7.4 were investigated. Swelling behavior differed between media and formulations. In pH 6.8 buffer, F02 showed a slow rehydration phase for the first 25 min, and then swelled rapidly until about 97 min, where the swollen beads exceeded the size of the corresponding fresh beads and continued to grow more slowly to reach roughly 142 % of its initial dry size after 8 hours (Figure 3a). F07 and F12 also swelled more at pH 6.8 than at pH 7.4; F07 reached the largest increase ( $\approx 136$  %), while all three formulations showed relatively less swelling in pH 7.4. The beads exhibited limited swelling in acidic medium (pH 1.2), except for a small initial expansion attributed to outer shell moisterization. Mechanistically, water first hydrates alginate's hydrophilic groups and then diffuses into pores, while ion exchange ( $\text{Na}^+$  in the medium replacing  $\text{Ca}^{2+}$  in the gel) relaxes chains and increases electrostatic

repulsion between carboxylates, causing the network to expand (Bajpai and Sharma 2004). In phosphate-containing buffers this process can be amplified because phosphate binds  $\text{Ca}^{2+}$  and promotes shell decoupling, which explains the turbidity sometimes seen in the medium and the faster disassembly under those conditions (Azad *et al.* 2020). The higher diameter change observed in pH 6.8 compared to pH 7.4 after 400 min (Figure 3b) can be attributed to differences in buffer ionic composition and ion–alginate interactions. The presence of monovalent ions in the pH 6.8 medium enhances  $\text{Ca}^{2+}$  ion exchange within the alginate network, weakening crosslinking and promoting greater water uptake compared to pH 7.4 buffer. These mechanisms explain why beads swell more in neutral-to-alkaline buffers and remain stable in strong acid. Within this system, HPMC likely acts as a hydrophilic diffusion barrier that increases network tortuosity and contributes to the sustained-release behavior. The practical consequence is that swelling, and the ease, with which the polymer network opens in a medium with specific pH, controls when and how fast eugenol can be released.

Release profiles in pH 6.8 (Figure 3c) show clear links to swelling. F02 released about 50 % of its eugenol within one hour and exceeded 95 % by 210 min. F07 started slower, accelerated near 120 min, and reached  $\approx 99$  % by 270 min. F12 gave the slowest profile, only  $\approx 25$  % released in the first 120 min,  $\approx 90$  % at 270 min and  $\approx 99$  % by roughly six hours. In short, higher polymer fraction and tighter crosslinking slow eugenol diffusion, while greater swelling speeds it up. Based on the kinetic fitting results for the three samples, the Korsmeyer–Peppas model best describes the release behavior, as it consistently shows the highest  $R^2$  values compared to first-order and Higuchi models, with  $n$  values of 0.62, 0.95 and 1.04 for the F02, F07 and F12 samples respectively. This indicates that eugenol release follows an anomalous transport mechanism (F02 and F07) or Case-II transport (F12) primarily controlled by swelling or polymer relaxation of the alginate matrix rather than simple diffusion. For applications needing extended delivery, such as colon-targeted systems, F12's profile is the most relevant (Uyen *et al.* 2020). These results offer practical levers to tune eugenol release for different uses.

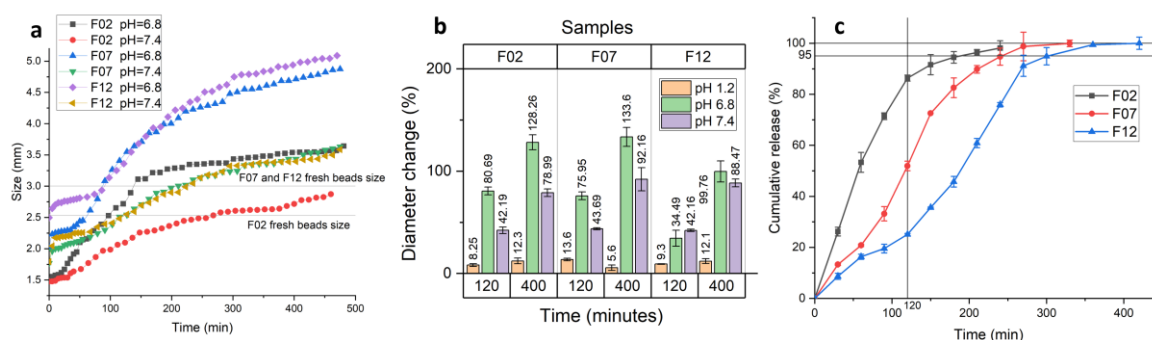


Figure 3: Swelling profiles for F02, F07 and F12 at pH 6.8 and 7.4 media (a), beads diameter change (%) comparative bars chart (b) and eugenol release profiles for F02, F07, and F12 runs in pH 6.8 buffer (c).

#### 4. Conclusions

Eugenol was encapsulated in alginate–HPMC beads prepared by ionic gelation. Needle size and drop height determined bead size where a 25-gauge needle positioned 6 cm above the gelling bath yielded the small beads with the narrowest size distribution. EEs across formulations ranged from 55.6 % to 78.8 %, with F02 (2 % w/v alginate, 5 % w/v  $\text{CaCl}_2$ ) giving the highest EE. LCs were about 4.6–11.4 %. Swelling tests showed minimal change in acidic medium (pH 1.2) and significant swelling at pH 6.8 and 7.4 media, consistent with ion-exchange driven network relaxation. Higher polymer fraction and stronger crosslinking controlled eugenol release for up to six hours. Surface porosity and drying affected shrinkage and release variability, and dry beads retained most of their eugenol over 150 days at room temperature. Moderate alginate levels combined with sufficient  $\text{Ca}^{2+}$  offer a good compromise between payload and stability, thus supporting the use of these beads for controlled eugenol delivery in food and pharmaceutical applications. Further investigation into the effects of other parameters and experimental modelling of the process could provide additional valuable insights into the use of this technique for the encapsulation of eugenol or other volatile actives.

#### Acknowledgments

The authors are grateful to "La Direction Générale de la Recherche Scientifique et du Développement Technologique (DGRSDT)" for supporting this work.

#### References

Abang, S., Chan, E.-S., and Poncelet, D., 2012. Effects of process variables on the encapsulation of oil in calcium alginate capsules using an inverse gelation technique. *Journal of microencapsulation*, 29 (5), 417–428.

- Ahmed, M.M., El-Rasoul, S.A., Auda, S.H., and Ibrahim, M.A., 2013. Emulsification/internal gelation as a method for preparation of diclofenac sodium-sodium alginate microparticles. *Saudi Pharmaceutical Journal*, 21 (1), 61–69.
- Azad, A.K., Al-Mahmood, S.M.A., Chatterjee, B., Wan Sulaiman, W.M.A., Elsayed, T.M., and Doolaanea, A.A., 2020. Encapsulation of black seed oil in alginate beads as a pH-sensitive carrier for intestine-targeted drug delivery: In vitro, in vivo and ex vivo study. *Pharmaceutics*, 12 (3), 1–26.
- Bagheri, L., Madadlou, A., Yarmand, M., and Mousavi, M.E., 2014. Spray-dried alginate microparticles carrying caffeine-loaded and potentially bioactive nanoparticles. *Food Research International*, 62, 1113–1119.
- Bajpai, S.K. and Sharma, S., 2004. Investigation of swelling/degradation behaviour of alginate beads crosslinked with Ca<sup>2+</sup> and Ba<sup>2+</sup> ions. *Reactive and Functional Polymers*, 59 (2), 129–140.
- Benavides, S., Cortés, P., Parada, J., and Franco, W., 2016. Development of alginate microspheres containing thyme essential oil using ionic gelation. *Food Chemistry*, 204, 77–83.
- Bowey, K., Swift, B.E., Flynn, L.E., and Neufeld, R.J., 2013. Characterization of biologically active insulin-loaded alginate microparticles prepared by spray drying. *Drug Development and Industrial Pharmacy*, 39 (3), 457–465.
- Chaieb, K., Hajlaoui, H., Zmantar, T., Kahla-Nakbi, A. Ben, Rouabhia, M., Mahdouani, K., and Bakhrouf, A., 2007. The chemical composition and biological activity of clove essential oil, *Eugenia caryophyllata* (*Syzygium aromaticum* L. Myrtaceae): A short review. *Phytotherapy Research*, 21 (6), 501–506.
- Chen, H.B., Wang, Y.Z., Sánchez-Soto, M., and Schiraldi, D.A., 2012. Low flammability, foam-like materials based on ammonium alginate and sodium montmorillonite clay. *Polymer*, 53 (25), 5825–5831.
- Davarcı, F., Turan, D., Ozcelik, B., and Poncelet, D., 2017. The influence of solution viscosities and surface tension on calcium-alginate microbead formation using dripping technique. *Food Hydrocolloids*, 62, 119–127.
- Faidi, A., Lassoued, M.A., Becheikh, M.E.H., Touati, M., Stumbé, J.F., and Farhat, F., 2019. Application of sodium alginate extracted from a Tunisian brown algae *Padina pavonica* for essential oil encapsulation: Microspheres preparation, characterization and in vitro release study. *International Journal of Biological Macromolecules*, 136, 386–394.
- Gülçin, I., 2011. Antioxidant activity of eugenol: A structure-activity relationship study. *Journal of Medicinal Food*, 14 (9), 975–985.
- Hu, L., Kong, D., Hu, Q., Yang, X., and Xu, H., 2017. Preparation and optimization of a novel microbead formulation to improve solubility and stability of curcumin. *Particulate Science and Technology*, 35 (4), 448–454.
- Jobdeedamrong, A., Jenjob, R., and Crespy, D., 2018. Encapsulation and Release of Essential Oils in Functional Silica Nanocontainers. *Langmuir*, 34 (44), 13235–13243.
- Kfoury, M., Auezova, L., Greige-Gerges, H., and Fourmentin, S., 2019. Encapsulation in cyclodextrins to widen the applications of essential oils. *Environmental Chemistry Letters*, 17 (1), 129–143.
- Lee, K.Y. and Mooney, D.J., 2012. Alginate: properties and biomedical applications. *Progress in polymer science*, 37 (1), 106–126.
- Maes, C., Bouquillon, S., and Fauconnier, M.L., 2019. Encapsulation of essential oils for the development of biosourced pesticides with controlled release: A review. *Molecules*, 24 (14), 2539.
- Partovinia, A. and Vatankhah, E., 2019. Experimental investigation into size and sphericity of alginate micro-beads produced by electrospraying technique: Operational condition optimization. *Carbohydrate polymers*, 209, 389–399.
- Pinto, E., Vale-Silva, L., Cavaleiro, C., and Salgueiro, L., 2009. Antifungal activity of the clove essential oil from *Syzygium aromaticum* on *Candida*, *Aspergillus* and dermatophyte species. *Journal of Medical Microbiology*, 58 (11), 1454–1462.
- Radünz, M., da Trindade, M.L.M., Camargo, T.M., Radünz, A.L., Borges, C.D., Gandra, E.A., and Helbig, E., 2019. Antimicrobial and antioxidant activity of unencapsulated and encapsulated clove (*Syzygium aromaticum*, L.) essential oil. *Food Chemistry*, 276, 180–186.
- Ramos, P.E., Silva, P., Alario, M.M., Pastrana, L.M., Teixeira, J.A., Cerqueira, M.A., and Vicente, A.A., 2018. Effect of alginate molecular weight and M/G ratio in beads properties foreseeing the protection of probiotics. *Food Hydrocolloids*, 77, 8–16.
- Santagapita, P.R., Mazzobre, M.F., and Buera, M.P., 2011. Formulation and drying of alginate beads for controlled release and stabilization of invertase. *Biomacromolecules*, 12 (9), 3147–3155.
- Sherry, M., Charcosset, C., Fessi, H., and Greige-Gerges, H., 2013. Essential oils encapsulated in liposomes: A review. *Journal of Liposome Research*, 23 (4), 268–275.
- Soliman, E.A., El-Moghazy, A.Y., El-Din, M.S.M., and Massoud, M.A., 2013. Microencapsulation of Essential Oils within Alginate: Formulation and in Vitro Evaluation of Antifungal Activity. *Journal of Encapsulation and Adsorption Sciences*, 03 (01), 48–55.
- Uyen, N.T.T., Hamid, Z.A.A., Tram, N.X.T., and Ahmad, N., 2020. Fabrication of alginate microspheres for drug delivery: A review. *International Journal of Biological Macromolecules*, 153, 1035–1046.
- Ward, F.M., Hanway, W.H., and Ward, R.B., 2005. Food gums: Functional properties and applications. *Handbook of Food Science, Technology, and Engineering - 4 Volume Set*, 149 (3), 2448–2463.